Geophys. J. R. astr. Soc. (1974) **39**, 11–28.

A New, Theoretically Tractable Earthquake Model*

John A. Whitehead and Roger F. Gans

(Received 1974 June 4)†

Summary

In this paper we explore the advantages gained in discussing stick-slip-like models in the context of simple mathematically-continuous friction laws. One such law is chosen and analysed in detail. ' Quaking behaviour ' is observed for this mathematical model and the parameters governing its behaviour are found to be two dimensionless numbers, both of which are smaller than 1 for behaviour most like earthquakes. A laboratory realization of the mathematical model is described and is observed to exhibit quaking behaviour.

Introduction

Modern studies of earthquake dynamics have centred around a number of approaches. The largest class of studies concern direct observations of the physical processes which accompany earthquakes such as stress waves, electric or magnetic effects, groundwater changes, surface tilt, morphological displacement and the like. A second class deals with laboratory measurements of the mechanical properties of the earth materials. In the course of these studies certain models of earthquake processes have emerged.

Generally, these models are described by equations whose terms are so complicated as to defy rational analysis, presumably in order to be geologically realistic. A discussion of this work is beyond the scope of this paper. The reader is referred to a review paper by Byerlee (1970) for details of the largest school, that of stick-slip.

Here, we attempt to put such ideas into their simplest theoretical forms. An inherent requirement is that the resulting equations must possess tractable solutions. The practical aspects of earthquake prediction and control are relegated to secondary roles; first priority has been given to utilizing simple *continuous* mathematical functions.

As will become clear during the course of this work, the crucial decision of the modeler is his choice of a law to govern the resistance of the material to motion or deformation. The study of such laws is called rheology, and we will use an abbreviated nomenclature, ' rheology ' standing for the resistance law. The power of our method, and the justification for departing from ' geological reality ' is that the simple law we use reduces to stick-slip in one limit, and the mechanism of Griggs & Baker (1969) in another limit. It possesses the further merit that a laboratory model can be built, and a crude version of such a model is described below.

* Contribution No. 3281 of the Woods Hole Oceanographic Institution.

† Received in original form 1974 March 19.

There is another reason for this work: processes which store and suddenly release large amounts of energy occur elsewhere in nature. Some examples are mud-slides, turbidity currents, wet and dry avalanches, glacial surges, and the proposed neutron star collapse. By theoretically formulating such problems, we can hope to categorize sudden release mechanisms into various classes, and thereby gain a deeper understanding of their basic nature.

This study indicates that two dimensionless numbers are needed: one expressing the ratio of rapid sliding friction to slow deformational friction, and another expressing the role of inertia. Both are necessarily non-zero for a well-behaved solution. For solutions most like earthquakes both numbers are small. We point out that this is a special case of the more general circumstance, that one more parameter is required than the number required in the ' rheology '.

The plan of the paper is as follows: In Section 2 we derive equations governing the sliding of a block towed by a spring. These equations contain an arbitrary function representing the friction between the block and its surroundings. We choose a particular function which we believe is both simple and relevant to previous geophysical modelling.

In Section 3 detailed analysis of the system is carried out, and in Section 4 a physical device which obeys our friction law is described. Finally some discussion is given in Section 5.

2. Formulation

The ' existing ' models of earthquake processes, whether the basic stick-slip (see Byerlee 1970) or more complex models created to study statistics (see Burridge & Knopoff 1967) have as basic components a mass-spring system, as in Fig. 1.

The mass M lies on a flat surface, and is attached to a spring which is pulled along at a velocity u_0. If the spring is linear, with spring constant k, and u denotes the velocity of the block, we can write a second order differential equation which governs the behaviour of the system, namely,

$$M\ddot{u}+\frac{dg}{du}\dot{u} = k(u_0-u), \tag{1}$$

where dots denote differentiation with respect to time, and $g(u)$ is the force caused by friction between the block and the surface. *The results of any given analysis depend on the choice of* $g(u)$.

It is clear that the equation admits the solution $u \equiv u_0$. Whether this solution is stable to infinitesimal disturbances depends on the sign of $g'(u_0)$, where prime denotes the derivative with respect to u. If $g'(u_0) < 0$ the system is unstable to infinitesimal disturbances; if $g'(u_0) > 0$ it is stable.

The specification of a force law for the system shown in Fig. 1 is complicated by the fact that no correct law valid for sliding friction is available. Moreover the same situation holds for earthquakes, so any worker dealing with equations like (1) is necessarily bound to invent some $g(u)$. The stick-slip school tends to use heuristic

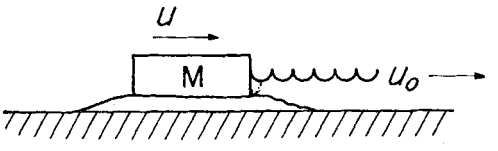

FIG. 1. The sliding block model.

argument to create forbiddingly complicated functions. Burridge & Knopoff chose the very simple $g(0) = g_1$ and $g(u) = g_2$, $u \neq 0$, with $g_1 > g_2$.

Neither of these is particularly attractive. The former choice generally contains too many parameters for rational analysis, and the second leads to mathematical difficulties because of the discontinuity. Therefore we wish to put forward our own $g(u)$, which is, in a sense to be discussed below, the simplest continuous g leading to ' quaking ' behaviour:

$$g(u) = \frac{\mu u}{d_0 + \beta u^2}. \tag{2}$$

The friction law represented by (2) has the further advantage that it is approximately obeyed by a laboratory device described below, so that, unlike the sliding block modellers, we are capable of looking at an experimental apparatus that obeys a continuous force law that we can write down, and therefore we can analyse our basic building block theoretically.

While it is not directly relevant to the work reported here, we can note that our friction law bears qualitative resemblance to some experimental results on sliding friction. In this connection we cite Rabinowitz (1965) for steel sliding on indium and lead, Bowden & Freitag (1958) for metal sliding on diamond, Bowden & Persson (1961) for steel on ' contaminated ' glass, and Grosch (1963) for various types of rubber on rough and smooth surfaces. In all of these results the friction coefficient increases with increasing sliding speed up to a maximum and then decreases with increasing sliding speed beyond the value at the maximum.

In what sense is $g(u)$ the ' simplest force law ' ? Any $g(u)$ allowing periodic (but not sinusoidal) solutions to (1) would serve. We begin by asserting that rational functions are simpler than irrational or transcendental functions. This is in part a matter of taste. Then given a rational function

$$f(u) = \frac{P_n(u)}{Q_m(u)},$$

where P_n and Q_m are polynomials of degree n and m, respectively, we call it simple accordingly as n and m are separately small.

The function must be odd and everywhere bounded, to make physical sense. Infinite drag at finite velocity makes no sense. Nor does ' anisotropic ' drag. (The latter might be useful in a geophysical context, however.) The simplest such function is $g(u) \propto u$, which leads to a linear equation, exactly solvable, the solution to which either decays to $u = u_0$, or grows exponentially without bound. The next simplest model is that which we have taken.

We are now in a position to derive the equations which lead to (1), and to cast them in a more convenient non-dimensional form. We let F be the force in the spring, and then, if the spring be linear, we have

$$\dot{F} = k(u_0 - u). \tag{3}$$

The acceleration of the mass, plus the drag force, must equal the spring force:

$$M\dot{u} + g(u) = F, \tag{4}$$

where $g(u)$ is given by equation (2).

Differentiating (4) with respect to time and substituting (3) leads to (1). It will be convenient, however, to retain the formulation in terms of a pair of coupled first order equations.

We non-dimensionalise the system using u_0 as the unit of velocity, $\mu/\beta u_0$ as the

unit of force and $\mu/(\beta u_0{}^2 k)$ as the unit of time. The system is then described in terms of two non-dimensional numbers

$$m = \frac{M\beta^2 u_0{}^4 k}{\mu^2}, \qquad \alpha^2 = \frac{d}{\beta u_0{}^2}, \tag{5}$$

representing inertia and the variability of friction respectively. In terms of these the governing equations are

$$\left.\begin{aligned} \dot{F}' &= 1-u', \\ m\dot{u}' + \frac{u'}{\alpha^2+u'^2} &= F' \end{aligned}\right\} \tag{6}$$

where primes have been used to denote dimensionless quantities. These primes are no longer necessary and so will be deleted in Section 3 following, in which we analyse the system (6). We will first outline the behaviour of our rehology in the context of previous models.

The stick-slip idealization imagines no motion until a critical force is reached, and then sliding begins with a fixed value of friction, independent of sliding velocity. In our model there is initially no resistance to slip, but the friction increases like $u\alpha^{-2}$, which can be quite rapid for small α. The friction attains a maximum value at $u = \alpha$, and then drops to zero as $u \to \infty$. Fig. 2 shows friction *vs* u for stick-slip and our friction function. (Our model is in some respects more realistic than the simple stick-slip model, but the question of which is most realistic is difficult to answer.)

There is also an analogy between equation (6) and the mechanism of deep earthquakes proposed by Griggs & Baker for deep focus earthquakes, which is:

(1) Material is viscous with a temperature-dependent viscosity.

(2) When flow exceeds a certain limit, the material heats up due to internal friction and becomes less viscous.

This results in an unstable feedback mechanism releasing elastic energy as an earthquake.

A viscous friction law states that resistance to motion is proportional to strain rate. If we imagine a thin layer of viscous material, of thickness d beneath our block, then we have the force law

$$g_v(u) = \frac{\mu(T)}{d}\, u, \tag{7}$$

where $\mu(T)$ is a temperature-dependent coefficient of viscosity.

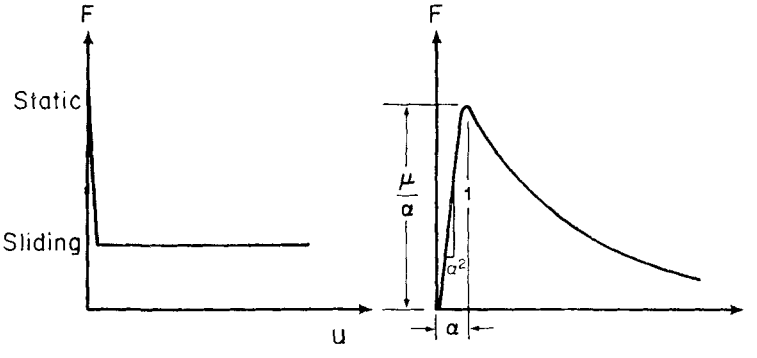

FIG. 2. Comparison of stick-slip (left) with the proposed rheology (right).

We then write the viscous version of (3) and (4) as

$$\left.\begin{aligned} \dot{F} &= k(u_0 - u), \\ M\dot{u} + \mu(T)u/d &= F. \end{aligned}\right\} \tag{8}$$

A third equation is needed to relate the temperature dependence of μ to the motion.

The function $\mu(T)$ will be analytic, and the first two terms in its Taylor series about T_0 are

$$\mu \approx \mu_0 - \mu_1(T - T_0) + \ldots. \tag{9}$$

The constant μ_1 is positive.

We assume a model in which the temperature difference, $T - T_0$, between the layer and its surroundings is linearly proportional to the heat generated, which can be approximated by $\mu\,(u^2/d^2)$:

$$C(T - T_0) = \mu \frac{u^2}{d^2}, \tag{10}$$

where C is a proportionality constant. $T - T_0$ is eliminated using (9), to yield

$$\mu = \frac{\mu_0/C}{1 + \dfrac{\mu_1}{Cd^2}\, u^2}. \tag{11}$$

Thus we have created a $g(u)$ of the form assumed.

We now proceed to discuss the behaviour of the mathematical model. We will first consider the question of the infinitesimal instability of the only steady-state solution. This occupies Section 3 to equation (14). We then discuss a singular solution in the limit $m \to 0$, which occupies the text through equation (17). The remainder of Section 3 is devoted to a numerical exploration of periodic solutions for the infinitesimally unstable case of $\alpha = \frac{1}{2}$ and for various values of m.

In Section 4 directly following we discuss a physical device which obeys our force law. The discussions in Sections 3 and 4 are essentially independent and may be read in any order.

3. Analysis

In this section we will discuss the system (6) with a view to understanding its behaviour as a function of m and α. We note first that the system admits only one time independent solution, namely,

$$u = 1,\ F = (1 + \alpha^2)^{-1}. \tag{12}$$

If this solution be perturbed according to the following

$$u = 1 + \varepsilon u_1, \quad F = (1 + \alpha^2)^{-1} + \varepsilon F_1,$$

and terms linear in ε retained, we find the equations

$$\left.\begin{aligned} \dot{F}_1 &= u_1, \\ m\dot{u}_1 + (\alpha^2 - 1)\, u_1 &= F_1, \end{aligned}\right\}$$

which can be reduced to

$$m\ddot{u}_1 + (\alpha^2 - 1)\,\dot{u}_1 + u_1 = 0, \tag{13}$$

which admit solutions proportional to exp (pt), where

$$p = \frac{1-\alpha^2}{2m}\left\{1 \pm \left[1 - \frac{4m}{(1-\alpha^2)^2}\right]^{\frac{1}{2}}\right\}. \tag{14}$$

If $\alpha^2 < 1$ the solutions are growing exponentials; the time-independent system is unstable. If $\alpha^2 > 1$, the solutions are decaying exponentials; the system is stable to infinitesimal perturbation. We note also that if

$$\frac{4m}{(1-\alpha^2)^2} \gg 1,$$

which will always be true in the neighbourhood of $\alpha = 1$, the solutions are nearly sinusoidal with period $m^{\frac{1}{2}}$. The solution hints at the conclusion one might arrive at intuitively: the smaller m, the quicker the approach to whatever the final state.

We have been unable to find any time-dependent closed form solutions to (6). We can, however, find an exact solution which is valid when $m \equiv 0$. This solution is likely to be singular, as the order of the differential system is lowered in this limit, and it is necessary to be circumspect about the application of this result. We shall discuss this point further after this solution is presented.

When $m = 0$ the system (6) can be reduced to

$$\frac{\alpha^2-u^2}{(\alpha^2+u^2)^2}\dot{u} = 1-u, \tag{15}$$

which can be integrated to give an implicit formula for u, namely,

$$(t-t_0) = \frac{u-\alpha^2}{(1+\alpha^2)(\alpha^2+u^2)} + \frac{1-\alpha^2}{2(1+\alpha^2)^2} \times \log\frac{(1-u)^2}{(\alpha^2+u^2)} - \frac{2\alpha}{(1+\alpha^2)^2}\tan^{-1}\left(-\frac{u}{\alpha}\right). \tag{16}$$

t_0 is a constant of integration.

Notice that $t \to \pm\infty$ as $u \to 1$ accordingly as $\alpha^2 \gtrless 1$, and that there is a periodicity arising from the $\tan^{-1}$ term. This characteristic period is

$$\frac{2\pi\alpha}{(1+\alpha^2)^2},$$

or, in dimensional form,

$$T_\alpha = \frac{2\pi\alpha\mu}{\beta u_0{}^2(1+\alpha^2)^2}. \tag{17}$$

One defect of the solution (16) which can be recognized directly from the equation is that u can go to infinity in a finite time. The solution is plotted for $\alpha = \frac{1}{2}$ in Fig. 3. The indicated discontinuities arise because time must always increase; the solution we have obtained is periodic with a calculable period and has a finite negative amplitude, but an infinite positive amplitude.

To interpret this solution, and to assess the meaning of instability further, it becomes necessary to deal with the full non-linear system directly. Exact solutions are not available, but numerical integration is practicable, and provides proof, for

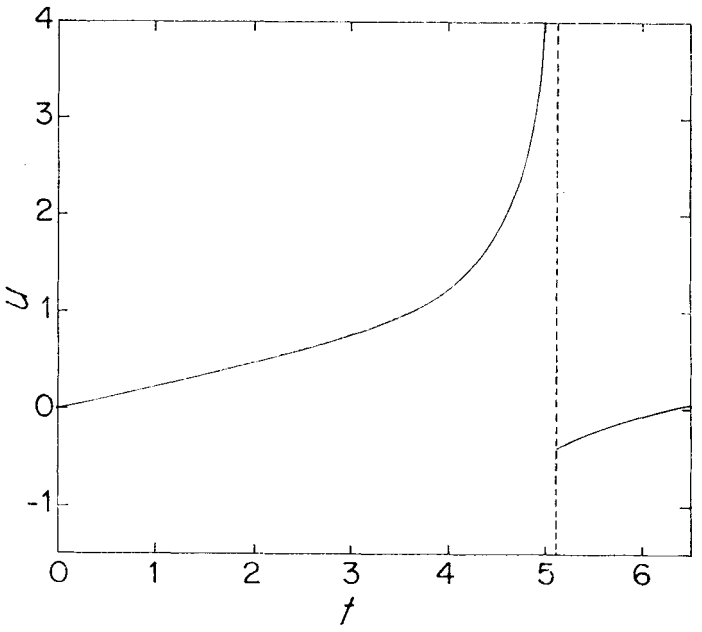

FIG. 3. Solution to the equation (15) for $\alpha = \frac{1}{2}$, $m = 0$ (singular solution).

all the cases we have considered, of the existence of periodic solutions.

A common technique for dealing with non-linear equations of this sort is to work on the phase plane—a plane defined by the values of each variable. Points where the derivatives vanish are called critical points; here there is only one critical point, at $(u, F) = (1, (1+\alpha^2)^{-1})$. It will be convenient to centre the critical point in the phase plane, therefore we define

$$\left.\begin{aligned} x &= F-(1+\alpha^2)^{-1}, \\ y &= u-1, \end{aligned}\right\} \tag{18}$$

and write our system as

$$\left.\begin{aligned} \dot{x} &= -y, \\ \dot{y} &= \frac{1}{m}\left\{x+\frac{1}{1+\alpha^2}-\frac{1+y}{(1+y)^2+\alpha^2}\right\}, \end{aligned}\right\} \tag{19}$$

which has its critical point at (0, 0).

Whether a point in the phase plane approaches or leaves the centre depends upon the sign of $x\dot{x}+y\dot{y}$, proportional to the rate of change of the square of the distance from the centre. This quantity is

$$x\dot{x}+y\dot{y} = \frac{y}{m}\left\{(1-m)x+\frac{1}{1+\alpha^2}-\frac{1+y}{(1+y)^2+\alpha^2}\right\}, \tag{20}$$

which vanishes at $y = 0$ and on the curve

$$x = \frac{1}{m-1}\left[\frac{1}{1+\alpha^2}-\frac{1+y}{(1+y)^2+\alpha^2}\right] = \frac{1}{1-m}x_1(y) \tag{21}$$

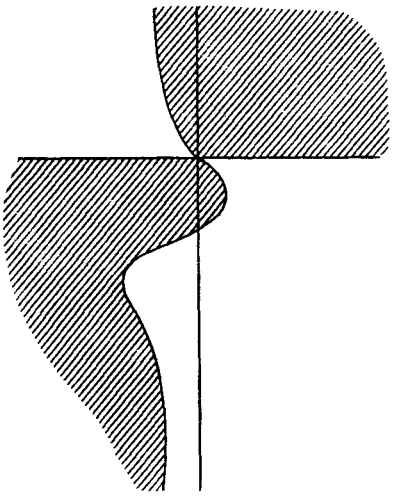

FIG. 4. The phase plane for m, $\alpha^2 < 1$. Shaded areas are for $x\dot{x}+y\dot{y}$ and clear areas for $x\dot{x}+y\dot{y} < 0$.

so that the phase plane is divided into four segments, in two of which x^2+y^2 increases and in two of which it decreases. A typical situation with $\alpha < 1$ and $m < 1$ is sketched in Fig. 4.

We now ask whether periodic solutions can exist for the unstable ($\alpha < 1$) case. This is equivalent to asking whether the system (19) has a limit cycle, a periodic solution to which the system tends as time increases.

We have been unable to prove this in general, but we have derived a sufficient condition for the existence of a limit cycle, and in all the cases we have checked this condition has been satisfied. We state the sufficient condition as: if one can integrate the system (19) numerically, using a marching scheme, around a complete circuit within which the curvature is of one sign, and finish inside the initial point, then a limit cycle exists. (This is equivalent to the Poincaré–Bendixson criterion.) Our proof that this condition is sufficient and satisfied is somewhat tedious, so it has been relegated to an appendix.

In order to display the behaviour of solutions as a function of m, we fixed $\alpha = \frac{1}{2}$ and performed the numerical integrations necessary to establish limit cycles for $m = 4, 1, \frac{1}{4}, 1/64$. These computations yielded solutions which appear quite near the actual limit cycle, and the resulting velocity variations can be compared with our already-obtained $m = 0$ (singular) limit. Fig. 5 shows the sample trajectories. The $m = 4$ calculation has been sufficiently extended to establish the existence of a limit cycle, but we do not think the resulting curve is very close to the limit cycle. We feel the others represent the limit cycles within the accuracy of the graphical representation. (The computation scheme was a simple Euler marching scheme using the formulae

$$x_{n+1} = x_n - y_n\,\Delta t,$$

$$y_{n+1} = y_n + \frac{1}{m}\left\{x_n + \frac{1}{1+\alpha^2} - \frac{1+y_n}{(1+y_n)^2+\alpha^2}\right\}\Delta t,$$

varying Δt during the computation so as to stay within the permitted band* near $x = x_1$.)

* The meaning of *permitted band* is clear from the proof in the Appendix.

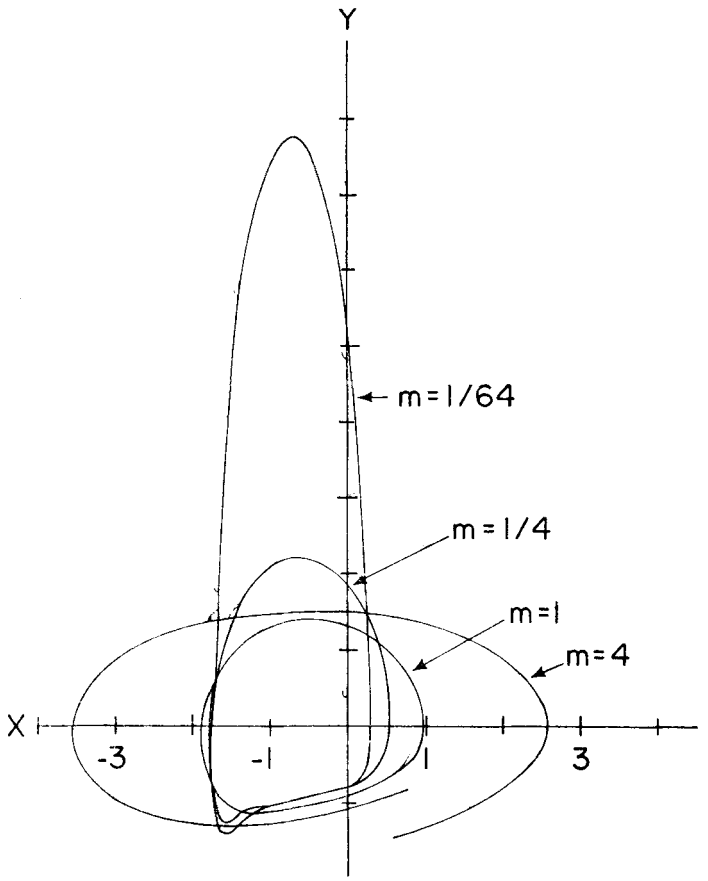

FIG. 5. Sample trajectories at $\alpha = \frac{1}{2}$ and for $m = 4, 1, \frac{1}{4}, 1/64$.

What can we say in general? The velocity patterns obtained range from nearly sinusoidal for larger m to more sharply-spiked distributions resembling that of Fig. 3 as $m \to 0$.

Large values of m give nearly circular tracks, representing almost sinusoidal motion. The period of such motion is $0(m^{\frac{1}{2}})$. Because earthquakes are quite asymmetrical in time—the quake being of very short duration compared to the build-up time—we feel that the small m limiting case is most directly relevant. One might be tempted to conjecture that inertial effects are relatively unimportant for real earthquakes and that the observed periodicities may be associated with the rheology.

When m is small its role is to limit the magnitude of the maximum response. (Remember that this was unbounded when m was set equal to zero.) An estimate of this magnitude can be constructed using the following physical arguments:

Consider the system to be moving slowly such that $\alpha^2 \ll u \ll \alpha < 1$. (The reader may wish to refer to a typical calculation here. Fig. 6 shows ' u ' vs time for $m = 0.1$ and $\alpha^2 = 0.04$.) The force balance is between the spring force and the viscous drag. The spring force increases nearly linearly with time until a time $t = \frac{1}{2}\alpha$ when it reaches the maximum resistive force possible: $\frac{1}{2}\alpha$. The velocity is approximately α. Additional increments in spring force added because the driving motion is still faster than the driven motion, can only be balanced inertially. The acceleration thus increases and the velocity increases dramatically. When this happens the frictional forces are

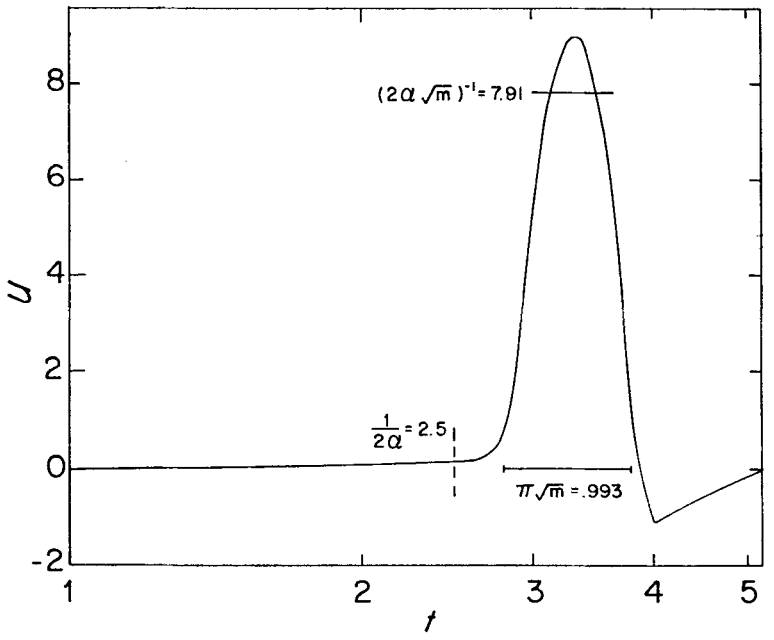

FIG. 6. Velocity as a function of time for $m = 0{\cdot}1$, $\alpha^2 = 0{\cdot}04$.

negligible and the system is essentially a mass-spring system with a half-period, or ' quake time ', of $(\pi\sqrt{m})^{-1}$.

The maximum velocity, u_m can be estimated by balancing the maximum force against the acceleration. The result is approximately $u_m = 1/(2\alpha\sqrt{m})$.

The above discussion applies only to $\alpha < 1$. We have proved the system stable to infinitesimal perturbations when $\alpha > 1$. We have not proved it stable for all disturbances for $\alpha > 1$, however, in view of the simplicity of the system, and the experimental evidence to be presented next we believe it to be absolutely stable when $\alpha > 1$.

4. A laboratory model

In this section we describe a laboratory device which obeys approximately a force law which is of the same form as that explored above. We indicate the possibility of constructing a model which obeys such a law much more precisely.

A diagram of the model is shown in Fig. 7. Starting from the bottom, a motor winds the lower end of a spring at a constant speed. The upper end of the spring is attached to a vertical shaft with an attached horizontal disk lying in a pan of glycerine. The disk is free to slide up and down the shaft and is attached to a speed governor.

The governor is a pair of weights at the end of pivoted arms. They are thrown out by centrifugal forces and kept down by gravity. The net effect of this device is to make the distance between the disk and the bottom of the pan vary as the square of the rotation rate:

$$d = d_0 + \beta\omega^2.$$

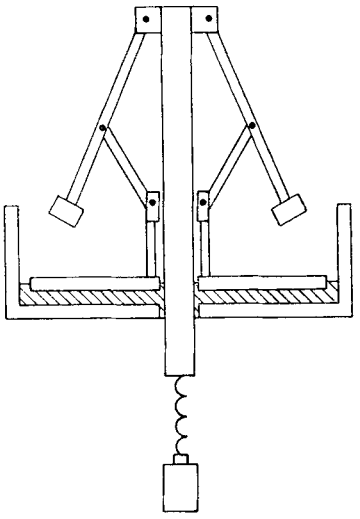

FIG. 7. Diagram of the experimental model. The glycerine is cross-hatched.

We establish the equations of motion under the hypothesis that the change in moment of inertia is small, so that

$$\frac{d}{dt}(I\omega) = I\frac{d\omega}{dt}.$$

This relation is moderately well satisfied during most of the motions. We will take this point up again below. First we describe the dynamics of the system and derive the relevant equations from which m and α^2 can be extracted.

The system can be viewed in terms of rotation rate and torque about the vertical axis, rather than velocity and force. The conservation of angular momentum is then

$$I\frac{d\omega}{dt} + g(\omega) = T \tag{22}$$

where I is the moment of inertia, ω the rotation rate, g the friction function and T the external torque of the spring. The rate of change of torque is proportional to the difference between the motor rotation rate and the disk rotation rate:

$$\frac{dT}{dt} = \xi(\omega_0 - \omega), \tag{23}$$

where ξ is a spring constant and ω_0 is the motor rotation rate.

The drag is caused by viscous dissipation in the glycerine. The torque associated with this drag is

$$T_d = 2\pi\mu \int_{r_1}^{r_2} r\frac{\partial v}{\partial z} r dr,$$

where μ is the viscosity, r_1 and r_2 the inner and outer radii limits of the disk, v the azimuthal velocity in the glycerine and z the co-ordinate normal to the disk.

We approximate $(\partial v/\partial z)$ by $\omega r/d$, d being the depth of the glycerine. Thus, after integrating and substituting for d, we obtain

$$g(\omega) = \tfrac{1}{2}\pi\mu\,(r_2^4 - r_1^4)\frac{\omega}{d_0 + \beta\omega^2}.$$

The reader can verify that, after non-dimensionalizing with angular velocity scale ω_0, time scale

$$\frac{\pi\mu(r_2^4-r_1^4)}{2\kappa\beta\omega_0^2}$$

and torque scale

$$\frac{\pi\mu(r_2^4-r_1^4)}{2\beta\omega_0}$$

the governing equations become

$$\left.\begin{aligned} \frac{dT'}{dt'} &= 1-\omega' \\ m\frac{d\omega'}{dt'} + \frac{\omega'}{\alpha^2+\omega'^2} &= T' \end{aligned}\right\} \tag{24}$$

where prime denotes non-dimensional quantities and

$$\alpha^2 = \frac{d_0}{\beta\omega_0^2}, \qquad m = \frac{4\omega_0^4 p^2 \kappa}{\mu^2(r_2^4-r_1^4)^2\pi^2}. \tag{25}$$

Thus we can hope to apply the theory developed above directly to this model.

Unfortunately the acutal device we have departs significantly from the ideal device we have described in two ways. First, most of the mass contributing to the moment of inertia is in the moving arms, so that the moment of inertia changes by nearly a factor of 20 during a quake sequence. Most of this change takes place in a shot space of time in the initial peak of a quake episode. The result is to transfer from a small m limit cycle to a large m domain with an initial condition not on the limit cycle. One cannot expect the limit cycle for either m to reflect accurately what the machine is attempting to do.

A second, and more serious difference is in the force law. For small d_0 there is clearly a process of sticking: the disk is hindered from rising by viscous forces, as well as being dragged by them. The effect of this is to extend the time scale greatly and to move the device off the limit cycle to the right, in the direction of increasing force.

Because of these effects neither the period length nor the maximum amplitude can be easily related to the theoretical results.

Despite these problems the parameters m and α^2 are still the major parameters governing the behaviour of the system. We expect qualitative resemblance between the theoretical curves and the experimental curves, and we expect the stability criterion to be obeyed by the experimental model.

To calculate m and α^2 we need to know a number of physical properties of the system:

The spring constant was measured directly using a spring scale, recording the torque for various numbers of turns of the spring. The value of the constant was found to be 3.4×10^4 dyne cm rad^{-1}.

The viscosity was measured in a Cannon–Fenske viscometer and converted to dynamic viscosity using handbook values for density. The value was taken as 9.6 poise.

The parameter group $\frac{1}{2}\pi(r_2^4-r_1^4)$ was calculated from the geometry of the disc ($r_2 = 9$ cm $r_1 = 5$ cm) as 9324 cm^4.

β was measured by recording height of the disk as a function of ω.

The system obeys a $\omega^{9/4}$ law more closely than a ω^2 law, and effective values of β run from less than 0.02 to more than 0.04 cm $(\text{rad s}^{-1})^{-2}$. We have adopted an 'average' value of 0.024, though the data regarding stability seem to indicate that, at least as far as stability is concerned, a value nearer 0.02, typical of slow rotation rates, is more appropriate.

Lastly, m was measured directly by winding the spring without glycerine in the pan, then suddenly releasing the disk. It was found to be 1.9×10^6 dyne $\text{cm}^{-1}\,\text{s}^2$ with the weights fully extended and 8.9×10^4 dyne $\text{cm}^{-1}\,\text{s}^2$ with the weights held in a down position. Similar values were obtained by calculation.

The height of the disk when there is no rotation, d_0, and the rotation rate ω_0 could be varied from 0.1 to 2 cm, and 0.1 to 4 rad s^{-1}, respectively, and hence the dimensionless numbers could be specified within limits: $0.2 < \alpha^2 < 4$, $m_{\max} \leqslant 1.2$, $m_{\min} \leqslant 0.056$.

The experimental procedure was as follows: The variable d_0 was set by raising or lowering the governor assembly, then locating the depth of the bottom of the disk from the bottom of the pan with a cathetometer. The speed of the driving motor was monitored with a stop watch to determine ω_0. Finally, rotation rate of the disk was recorded on a chart recorder using voltage from a generator attached to the shaft, and torque could be read directly from a torquemeter.

To the precision that the constants were measured, the stability of this model agreed qualitatively with the prediction in Section 2. The state $\omega = \omega_0$ was stable for α^2 greater than about 0.85, while it was unstable for values less than this and exhibited periodic time-dependent behaviour. An example of this behaviour can be seen in Fig. 8, which shows velocity as a function of time for a series of different values of α^2 with the parameter m (extended) = 1.22, m (contracted) = 0.057. These experiments were started from a zero initial condition, so the first part of the curve corresponds to a start time. We note that the system rapidly approaches a steady-slip condition for $\alpha^2 \gg 0.85$, but it wanders about a steady-slip condition as a decaying oscillation when α^2 is just slightly above the critical value. Since this is what the linear stability theory predicted, it is evidence that the system is not unstable to finite-amplitude perturbations in the neighbourhood of the critical value.

However, the period of oscillation of approximately 50 s is considerably larger than the period of the theoretical model which can be found from equation (14) for $\alpha^2 \simeq 1$ to be dimensionally $\sqrt{(M/k)}$ which is only a few seconds at most. Also, the decay time in the vicinity of $\alpha^2 \simeq \alpha$ crit appears to be longer than the theoretical prediction.

We believe that the principal cause of this is that the disk 'sticks' to the bottom of the container when d is small. This also appears to cause a much longer build-up time T for the fully developed quake sequence shown in the bottom of Fig. 8.

However, the laboratory model exhibits the qualitative behaviour, in the vicinity of $\alpha^2 = 1$, and in the sequence of its quake behaviour, i.e. a long viscous build-up time, and then an 'earthquake' release where the principal balance is between the elastic force F and inertia.

5. Concluding comments

This attempt to formulate and analyse the mechanics of earthquakes leads to a number of possibilities. Firstly it results in explicit statements about the role of certain parameters. For instance, behaviour most like earthquakes seems to be characteristic of $m \ll 1$. In this limit, the build up time is $1/2\alpha$ (dimensionless), or

$$\frac{\mu}{2\sqrt{(d_0\beta')}\,u_0 k}$$

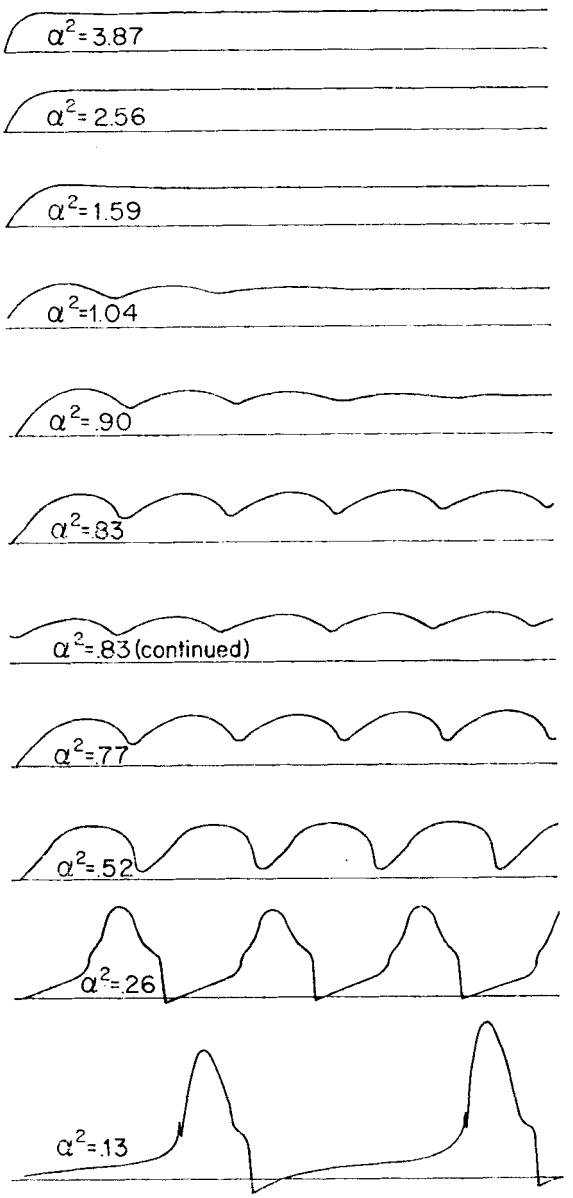

FIG. 8. Velocity (top) as a function of time for various values of α^2 and m (extended) = 1·22, m (contracted) = 0·057. Time scale 1 inch = 100 seconds.

(dimensional), the release time is $\pi\sqrt{m}$ (dimensionless) or $\pi\sqrt{(M/k)}$ (dimensional), and the ratio of release time to build up time is $2\pi\sqrt{(m)}\alpha$, or

$$2\pi\frac{\sqrt{(M\beta u_0{}^2 k d_0)}}{\mu}.$$

We will not attempt to assess what values of these parameters are most appropriate for various earthquake regions. We will note that the values of μ, $\beta u_0{}^2$ and d_0 would be difficult to estimate, while M and k may be easier to estimate. Without further justification we will note that this approach may possibly be fruitfully applied to other cataclysmic phenomena such as mudslides, wet avalanches, landslides, glacial surges or neutron star contractions.

Another possibility is to extend the formulation to include other relevant processes. Perhaps the most obvious possibility is to model the role of interstitial water in either or both of its two roles as a lubricant and as a dashpot. Burridge & Knopoff showed how the latter process contributes to the aftershock phenomenon, while the former process has recently received much attention in conjunction with detected earthquake precursors. A second extension could be to introduce a spatial dependence. In such a problem properly formulated, singular fault regions could be expected. A third extension could be to analyse multiply-connected devices, and to adjust the elements of such systems independently.

We would like to close on a cautionary note. Deducing seismic mechanisms from earthquake observations is a geophysical inverse problem of immense complexity. It should be clear that one cannot deduce the physics from the observations, but only fit parameters to models. This is the situation in the common inverse problems in geophysics such as the deduction of the Earth's structure from global oscillations, but the latter is helped by a general agreement that linear elasticity is an appropriate model. Our problem is complicated by the lack of a generally agreed upon model; we do not claim that $g(u)$ as given above is necessarily the correct physical model.

J. A. Whitehead:
Department of Physical Oceanography,
Woods Hole Oceanographic Institution,
Woods Hole, Massachusetts 02543

R. F. Gans:
Department of Mechanical and Aerospace Sciences
University of Rochester
Rochester, New York

References

Bowden, F. P. & Freitag, E. H., 1958. *Proc. R. Soc. A*, **248,** 350–367.
Bowden, F. P. & Persson, P. A., 1961. *Proc. R. Soc. A*, **260,** 453–458.
Burridge, R. & Knopoff, L., 1967. *Bull. seism. Soc. Am.*, **57,** 341.
Byerlee, J. D., 1970. *Tectonophysics*, **9,** 475.
Griggs, D. T. & Baker, D. W., 1969. *Properties of matter under unusual conditions* 23–42, eds H. Mark and S. Fernbach, Interscience, New York.
Grosch, K. A., 1963. *Proc. R. Soc. A*, **274,** 21–39.
Rabinowitz, E., 1965. *Friction and wear of metals*, Chapter 4, 52–108, Wiley, New York.

Appendix

The sufficient condition for a limit cycle

It should be clear that the condition is sufficient. We choose a point in the phase plane and calculate dy/dx. We then step forward along the tangent line to a new position in the phase plane. Our new point lies on a trajectory which began outside the trajectory containing the first point. Because of the curvature property we will continually transfer to outside trajectories, so that if we are inside our original starting point after one circuit we have established that a series of trajectories spiral in. As the system is autonomous (no explicit appearance of t) no two trajectories can cross, and as the system is unstable at the origin, the trajectories cannot spiral in indefinitely, hence there must be a limit cycle.

We now proceed to the tedious task of finding a region within which the curvature behaves appropriately. Curvature is given by

$$\frac{\pm y''}{[1+y'^2]^{3/2}}$$

where the sign is positive if the arc length S increases with x and negative otherwise. Since the curves under consideration have S increasing counterclockwise we would choose the lower sign when $y > 0$ and the upper sign when $y < 0$ so that we can ask to find a region where $y'' < 0$.

To calculate y'' we note that $y' = \dot{y}/\dot{x}$,

$$y' = -\frac{1}{my}\{x - x_1(y)\} \tag{A1}$$

so that

$$y'' = \frac{1}{my^2}\, y'(x-x_1) - \frac{1}{my}(1 - x'_1\, y'). \tag{A2}$$

After some algebra we obtain

$$y^3\, y'' = -\frac{1}{m}\, y^2 - \frac{1}{m^2}(x-x_1)(x-x_2), \tag{A3}$$

where

$$x_2(y) = x_1 - y\frac{dx_1}{dy},$$

and we require $y^3\, y'' < 0$.

Clearly if $x > \max(x_1, x_2)$ or $x < \min(x_1, x_2)$ the requirement is satisfied. If x lies between x_1 and x_2 there will be a further constraint on y. The maximum value of the second term, for fixed y, is at $x = \frac{1}{2}(x_1 + x_2)$, and that value is

$$\frac{1}{4m^2}(x_1 - x_2)^2 = \frac{1}{4m^2}\, y^2 \left(\frac{dx_1}{dy}\right)^2, \tag{A4}$$

from which we derive the criterion

$$1 > 4\frac{1}{m}\left(\frac{dx_1}{dy}\right)^2, \tag{A5}$$

or

$$-2\sqrt{(m)}\{(1+y)^4+2\alpha^2(1+y)^2+\alpha^4\} < \alpha^2-(1+y)^2 < 2\sqrt{(m)}\{(1+y)^4+2\alpha^2(1+y)^2+\alpha^4\}. \quad \text{(A6)}$$

The left-hand criterion is relevant when $y > -1+\alpha$ or $y < -1-\alpha$, and we are assured of its satisfaction if

$$y < -1-\sqrt{2}m^{-\frac{1}{4}} \quad \text{or} \quad y > -1+\sqrt{2}m^{-\frac{1}{4}}.$$

In the band $-1-\alpha < y < -1+\alpha$ the right-hand criterion applies, and is always satisfied if $4m \geqslant \alpha-4$. If m is smaller, as it is in many useful applications, there is an oval region within the region defined by $x_1 < x < x_2$, $-1-\alpha < y < -1+\alpha$, within which the sign of yy'' is positive. We summarize the situation in Fig. 9.

One can arrive at the limitations of the ' bad region ' as follows. We let $x = x_1+\theta$, so that

$$y^3 y'' = -\frac{1}{m}y^2 - \frac{1}{m^2}\theta(\theta+x_1-x_2),$$

and then we ask that θ be such that

$$y^2 > \frac{1}{m}\theta(\theta+x_1-x_2).$$

This is clearly true for $\theta_0 = 0$ and it must hold up to the first zero of the quadratic equation formed by setting the inequality to an equality, which is:

$$\theta_0 = -y\frac{x_1'}{2}\left[1-\left(1+\frac{4m}{x_1'^2}\right)^{\frac{1}{2}}\right]. \quad \text{(A7)}$$

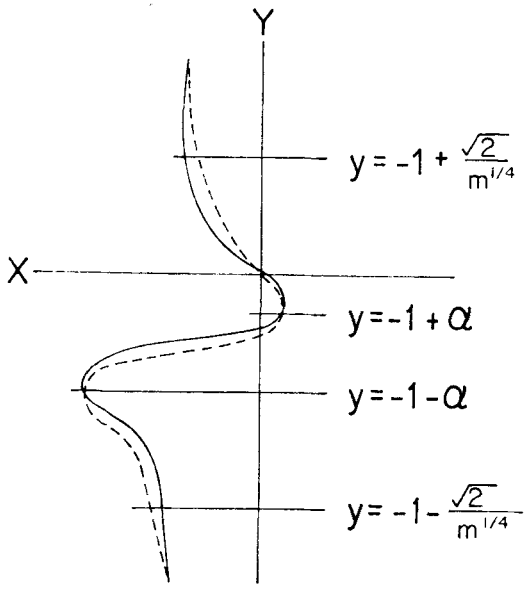

FIG. 9. Sketch of the regions where the criterion $yy'' < 0$ is met.
——— $x = x_1$, – – – – $x = x_2$.

The substitution $x = x_2 - \theta$ leads to exactly the same equation for θ_0 our band has a certain symmetry.

We see there are two types of complete circuit possible: one circling the outside all the singularities and the other running just past the ' bad region ' in the lower half plane. We have used this latter region in the analyses as it seems likely to be quite close to the genuine limit cycles.